Available online freely at www.isisn.org

Bioscience Research

Print ISSN: 1811-9506 Online ISSN: 2218-3973

Journal by Innovative Scientific Information & Services Network

RESEARCH ARTICLE BIOSCIENCE RESEARCH, 2023 20(4):956-970. **OPEN ACCESS**

The *In-vitro*investigation of antibacterialandantifungal potential of hybrid schiff base-urea and some of their complexes supported with *In-Silico* bioactivity docking approaches

Lotfi M. Aroua[1*,2,3], Ahmed N. Al-Hakimi[1,4], Mahfoudh A. M. Abdulghani[5,6] and Sadeq K. Alhag[7]

[1]Department of Chemistry, College of Science, Qassim University, Campus University, King Abdulaziz Road, Al-Malida, Buraydah, Qassim, Kingdom of **Saudi Arabia**
[2]Laboratory of Organic Structural Chemistry and Macromolecules, Department of Chemistry, Faculty of Sciences of Tunis, Tunis El-Manar University, El Manar I 2092, Tunis,**Tunisia**
[3]Carthage University; Department of Chemistry, Faculty of Sciences of Bizerte, 7021 Jarzouna, **Tunisia**
[4]Department of Chemistry, Faculty of Sciences, Ibb University, Ibb, **Yemen**
[5]Department of Pharmacology & Toxicology, Unaizah College of Pharmacy, Qassim University, 5919, Qassim**, Kingdom of Saudi Arabia**
[6]Pharmacology department, international Medical School, Management and Science University, Shah Alam, 40100, **Malaysia**
[7]Department of Biology, College of Science, Ibb University, **Yemen**

***Correspondence:** lm.aroua@qu.edu.sa. **Received 08 Sep., 2023, Revised: 16 October 2023, Accepted: 17 October 2023 e-Published: 18 October, 2023**

The reaction of *o*-phenylenediamine, 1-naphthyl isocyanate, and suitable aromatic aldehyde 4a-e produced urea-Schiff base derivatives 5a-e. The ligand HL (5d) was achieved from 2-hydroxynaphthaldehyde and employed to elaborate mononuclear complexes 6a-c from Metal Cu^{2+}, Cr^{3+}, and Co^{2+}. Analytical investigations indicate that the HL ligand interacts with metallic ions through an octahedral-shaped neutral monodentate, or monobasic chelator involved in azomethine nitrogen and a protonated/deprotonated oxygen atom of phenolic group. The elemental study of the complexes revealed that the ligand bonds metallic ions via 1:1 ratio in all complexes. The crystallin system of compounds 5d and 6a-c have monoclinic, tetragonal, and orthorhombic structures which correspond to urea-Schiff base, cobalt (6b), and copper (6a). The antimicrobial activity of the Schiff base-urea derivatives 5a-e and their complexes 6a-c was investigated. Cobalt complex (6b), demonstrated a significant antibacterial activity against gram positive bacteria *Staphylococcus aureus* (CP), *Enterococcus faecalis*, and *Staphylococcus aureus* (CP), *Enterococcus faecalis*, and *Staphylococcus aureus* (CN) (17 ± 3, 14 ± 2 and 13 ± 2 mm), which is equivalent to the standard reference drug Erythromycin. The minimum inhibitory concentration (MIC) of cobalt complex was also evaluated and the MIC value found 2.5 µg/mL, which was extremely close to the standard reference drug Erythromycin. The docking investigation of molecules 5a-e and 6a-c revealed binding energy values ranging from 8.9 to 11.7 kcal/mol. The most active molecules from experiments, 5e and 6b, interacted with the key amino acids of the tyrosyl tRNA-synthetase catalytic site. Gram-positive bacteria may be susceptible to the antimicrobial effects of the urea-Schiff base cobalt complex.

Keywords: Urea-Schiff base, antibacterial activity, antifungal activity, complexes, in silico docking study.

INTRODUCTION

Schiff base was considered as a vital and essential intermediate for the development of various metal complexes with antibacterial (Madani et al. 2020, Elneairy et al. 2023, Rezaei et al. 2023,Ceramella et al. 2022) and antifungal properties(Madani et al. 2020,Varshney et al. 2023, Borrego-Muñoz et al. 2023, Aroua et al. 2023).Schiff bases were recently revealed to be promising antibacterial agents.A new sulfonamide Schiff base and their nano complexes (Hosny et al. 2023),novel derivatives of isatin-based Schiff base (Hassan et al. 2023),triazole Schiff bases and their oxovanadium complexes (Sharma et al. 2023), Schiff base derived from chitosan (Omer et al. 2023), Schiff-base metal complexes coating built from natural products (Liang et al. 2023),complexes with Schiff bases derived from 5-fluorosalicylaldehyde(Liang et al. 2023)was recently reviewed as antibacterial agents.A number of investigations have been conducted to study

the curative effects of Schiff base against a range of bacteria, including Gram-positive *Staphylococcus epidermidis*(Hassan et al. 2019), *Micrococcus luteus* and *Staphylococcus aureus*(Erturk et al, 2020),*Bacillus subtilis, Clostridium sporogenes,* and *Micrococcus flavus* (Salihović et al. 2021). To assess the antibacterial properties of Schiff base, various Gram-negative bacteria, covering *Acinetobacter baumanni*(Messasma et al. 2023)*Bacillus cereus, Escherichia coli* and *Pseudomonas aeruginosa*(Gümü et al. 2020),*S. thyphymurium*(Yusuf et al. 2020), *Proteus hauseri, K. pneumoniae, Salmonella enterica* and *subsp. enterica* serovar*Enteretidis*(Salihovi´c et al. 2021)also were studied.

Targeted Schiff base scaffoldswas also explored for antifungal activities. A various of molecules owing Schiff base was promoted as antifungal agents covering indole Schiff base (Wang et al. 2022),novel silver complexes with sulfadoxine-salicylaldehyde Schiff base (Oliveira et Al. 2022), novel Schiff bases derived from L-tryptophan(Borrego-Muñoz et al. 2023), new chiral selenate Schiff base and their Pd complexes (PrabhuKumar et al. 2022), novel Schiff base 5-methyl-3-((5-bromosalicylideneamino)pyrazole and its transition metal complexes (Devi et al. 2023), ruthenium (III) complex derived from chitosan Schiff bases (Amirthaganesan et al. 2022), 1,2,4-Triazole Schiff base derivatives(Dong et al. 2023), (1E,2E)-N-(6-ethoxybenzo[d]thiazol-2-yl)-3-(furan-2-yl)prop-2-en-1-imine(Abu-Yamin et al. 2022),chitosan Schiff base (Heras-Mozos et al. 2022),curcumin and alanine-curcumin Schiff base (Layaida et al. 2022).

Multitude studies have been accomplishing to examine the antifungal properties of Schiff base against a variety of fungi, including strains of *Fonsecaea*, *Aspergillus*, *Candida*and particularly, *Cryptococcus* (Magalhães et al. 2020),*Botrytis cinerea, Fusarium oxysporum*f. sp. cucumerium Owen and *Phomopsis asparagi*(Chen et al. 2020),*CandidaAuris*(Hamad et al. 2021)*,Candida* strains (*C. Auris*TDG1912)*, Candida albicans* (NCPF3281 *and* NCPF3179), *Candida glabrata* (NCPF8018), *Candida krusei*(NCPF3876), *Candida tropicalis* (NCPF8760) and *Candida parapsilosis*(NCPF3209) (Chowdhary et al. 2020),*Aspergillus niger*and *Candida albicans* (Bhagwatrao et al. 2021),*Pseudomonas syringae*pv and *Acinetobacter*sp(Genchi et al. 2022).

Urea is an extraordinary family of target chemical compounds with varied applications in biological and coordination chemistry. Researchers are fascinated by urea-derived compounds, which have a wide range of biological functions and therapeutic applications. The urea molecule represents essential precursors in chemical and medical chemistry. Urea has the ability to create stable interactions of hydrogen with proteins of interest and receptors due to its unique structure. Furthermore, a targeted urea scaffold was used to find antimicrobial agents covering a novel pyrimidine derivatives with arylurea, thiourea and sulfonamide moieties(Keche et al. 2012), Novel arylurea derivatives of aryloxy (1-phenylpropyl) alicyclic diamines (Canale, et al. 2023),naphtho[2,1-b] furan derived triazole-pyrimidines(Roopa et al. 2023),thiazolyl-urea derivatives(Sroor et al. 2022), Urea-thiazole/benzothiazole hybrids with a triazole linker (Poonia, et al. 2022),novel benzothiazole-urea hybrids(Zha et al. 2022),and oligourea-based foldamers(Tallet et al. 2022).

Bacterial infections are getting more difficult to cure due to microorganisms' ability to develop resistance to antimicrobial drugs. The primary mode of action of antimicrobial drugs is generally classified. Mechanisms involve cell wall synthesis inhibition (e.g., beta-lactams and glycopeptide drugs), protein synthesis inhibition (macrolides and tetracyclines), nucleic acid synthesis inhibition (fluoroquinolones and rifampins), and metabolic pathway inhibition (sulfamethoxazole and trimethoprim). Bacteria membrane disruption (polymyxin B and daptomycin). Bacteria may be resistant to one or more kinds of antimicrobial drugs by nature, or they can develop resistance through de novo mutations or the transfer of resistance genes from other bacteria (Tallet et al. 2022).

Bacteria with acquired resistance genes can create enzymes that degrade antimicrobial medications, develop efflux systems that prevent drugs from reaching their intracellular targets, change drug targets, or decrease drug action. It is feasible that alternative metabolic pathways that interfere with medications can be generated. Bacteria can acquire new genetic material from resistant strains by conjugation, transformation, or transduction, and transposons frequently promote the integration of numerous resistance genes into the host genome or plasmid. Antimicrobial drug use places selection pressure on the evolution of resistant strains (Uddin et al. 2022).

The primary problem facing the global healthcare system is the creation of novel antimicrobial drugs that can treat bacteria disorders. A set of urea Schiff base hybrids 5a-e and urea-Schiff base complexes 6a-c was synthesized. In order to further explore and find novel structures with biological activities (Aroua et al. 2020, Aroua et al. 2022, Alminderej et al. 2021, Alorini et al. 2023, Ghrab et al. 2022) and to produce antimicrobial medicines we investigated the activities of Schiff base-urea and their complexes as potential antibacterial as well as antifungal agents.

MATERIALS AND METHODS

2.1. General details

All essential chemicals were obtained from recognized suppliers such as Sigma-Aldrich in the United States, Oxoid Ltd in the United Kingdom, and LobaChemie Pvt. Ltd. in India. Spectrometer Cary 600 type Agilent in the range of 400-4000 cm^{-1} were employed to recorded FT-IR spectra. An NMR spectrum of ^{1}H and ^{13}C was achieved using a Bruker Avance III HD 850 MHz NMR spectrometer at 850 and 213 MHz, respectively. Using DMSO d_6 as the

solvent, all spectra were collected and and referred to TMS. Chemical shifts are presented in parts per million (ppm) on a scale from a residual DMSO (2.50 ppm) internal reference for ^{1}H NMR spectra. Constant of coupling presented in Hz. In ppm, chemical shifts provided from the scale's center peak of dimethyl sulfoxide d_6 in ^{13}C NMR spectra. Elemental analysis of (CHNS/O) measurements was performed using a Thermo Fisher Scientific Flash Smart Elemental Analyzer. Stuart SMP30 apparatus was used to determine the melting points. The TLC were achieved on plates Silica Gel type 60 F254. All reagents were utilized without additional purification. Absolute ethanol was used in the synthesis of products. Unless otherwise specified, all reactions were carried out in oven-dried glassware.

Chemistry

Synthesis of aminourea (3):

10 mmol of *o*-phenylenediamine, dissolved in 10 mL of dichloromethane, was added a solution of 1-naphthylisocyanate (1.69g) in 35 mL of dichloromethane. The reaction was left to stirring at 25° C for 0.5 h. TLC was used to control the progression of reaction with hexane /diethyl ether (30/70). At the end, the reaction was cooled, filtered and the raw material was further recrystallized from ethanol.

Compound 3: White powder, yield: 90%; M.p. 280-282°C; IR (cm^{-1}) *v* : 3258 (NH), 1646 (C=O), 1606 (C=N); 1547 (C=C);^{1}H NMR (850 MHz, DMSO-d_6) δ(ppm): 8.85 (s, 1H, NH), 8.21-8.17 (m, 2H, NH+H$_{arom}$), 8.03 (dd, 1H, *J*= 7.6, *J*= 4.2 Hz, H$_{arom}$), 7.92 (d, 1H, *J*= 7.6 Hz, H$_{arom}$), 7.61-7.57 (m, 2H, H$_{arom}$), 7.55-7.53 (m, 1H, H$_{arom}$), 7.49-7.45 (m, 1H, H$_{arom}$), 7.40 (dd, 1H, *J*= 5.9, *J*= 5.1 Hz, H$_{arom}$), 6.86 (td, 1H, *J*= 8.5, *J*= 7.6 Hz, H$_{arom}$), 6.77 (dd, 1H, *J*= 7.6 Hz, *J*= 4.25 Hz, H$_{arom}$), 6.60 (td, 1H, *J*= 8.5, *J*= 7.6 Hz, H$_{arom}$), 4.85 (s, 2H, NH$_2$); ^{13}C NMR (213 MHz, DMSO-d_6) δ (ppm): 159.99, 141.39, 135.17, 134.22, 131.70, 128.88, 126.39, 125.20, 124.90, 124.25, 122.99, 121.90, 121.90, 117.90, 117.41, 117.29, 116.34. Elem. Anal. for $C_{17}H_{15}N_3O$: calcd C, 73.63; H, 5.45; N, 15.15; O, 5.77; found C, 73.65; H, 5.43; N, 15.17; O, 5.75.

Synthesis of urea-Schiff bases (5a-e):

Amino-urea**3** (10 mmol) was dissolved in ethanol (20 mL) and suitable arylaldehyde 4 (15 mmol) in 20 mL of ethanol was added in a 100 mL round bottom flask. The mixture was stirred at ambient temperature for 30 minutes before being heated under reflux (12-20h). Mixture of ether/petroleum ether: 70/30 was employed to monitor the reaction progress using TLC. The content of reaction was filtered and the solid material was recrystallized from ethanol.

Compound (5a): Yellow solid, yield: 78%; M.p. 218-220°C; IR (cm^{-1}) *v* : 3284 (NH), 1642 (C=O), 1588(C=N); 1532(C=C);^{1}H NMR (850 MHz, DMSO-d_6) δ(ppm): 9.50 (s, 1H, NH), 8.80 (s, 1H, NH), 8.73 (s, 1H, CH=N), 8.28 (dd, 1H, *J*= 8.5 Hz, *J*= 7.6, H$_{arom}$), 8.17 (d, 1H, *J*= 8.5 Hz, H$_{arom}$), 8.06 (d, 2H, *J*= 8.5 Hz, H$_{arom}$), 7.96 (d, 1H, *J*= 8.5 Hz, H$_{arom}$), 7.87 (d, 1H, *J*= 8.5 Hz, H$_{arom}$), 7.74 (d, 1H, *J*= 8.5 Hz, H$_{arom}$), 7.65-7.63 (m, 2H, H$_{arom}$), 7.59-7.58 (m, 1H. H$_{arom}$), 7.56-7.55 (m, 1H, H$_{arom}$), 7.51 (t, 1H, *J*= 8.5 Hz, H$_{arom}$), 7.36 (dd, 1H, *J*= 8.5, *J*=7.6 Hz, H$_{arom}$), 7.23 (t, 1H, *J*= 7.6 Hz, H$_{arom}$), 7.03 (td, 1H, *J*= 8.5, *J*= 7.6 Hz, H$_{arom}$); ^{13}C NMR (213 MHz, DMSO-d_6) δ (ppm): 159.0, 158.9, 153.52, 138.51, 136.74, 135.34, 134.54, 134.30, 131.26, 129.39, 128.80, 127.84, 127.65, 126.50, 126.34, 126.20, 124.45, 122.68, 122.48, 120.32, 119.36, 117.83. Elem. Anal. for $C_{24}H_{18}ClN_3O$: calcd C, 72.09; H, 4.54; Cl, 8.87; N, 10.51; O, 4.00; found C, 72.13; H, 4.52; Cl, 8.83; N, 10.53; O, 3.99.

Compound (**5b):** Yellow solid, yield: 88%; M.p. 231-232°C; IR (cm^{-1}) *v*: 3281(NH), 1642(C=O), 1589(C=N); 1544(C=C); ^{1}H NMR (850 MHz, DMSO-d_6) δ(ppm): 9.47 (s, 1H, NH), 8.96(s, 1H, NH), 8.74 (s, 1H, CH=N), 8.34 (d, 1H, *J*= 6.8 Hz, H$_{arom}$), 8.29 (d, 1H, *J*= 7.6 Hz, H$_{arom}$), 8.15 (d, 1H, *J*= 8.5 Hz, H$_{arom}$), 7.94 (d, 1H, *J*= 7.6 Hz, H$_{arom}$), 7.88 (d, 1H, *J*= 7.6 Hz, H$_{arom}$), 7.82 (d, 1H, *J*= 1.7 Hz, H$_{arom}$), 7.71 (d, 1H, *J*= 7.6 Hz, H$_{arom}$), 7.65 (d, 1H, *J*= 7.6 Hz, H$_{arom}$), 7.58 (t, 1H, *J*= 7.6 Hz, H$_{arom}$), 7.55 (t, 1H, *J*= 7.6 Hz, H$_{arom}$), 7.40 (t, 1H, *J*= 8.5 Hz, H$_{arom}$), 7.35 (d, 1H, *J*= 7.6 Hz, H$_{arom}$), 7.28 (t, 1H, *J*= 7.6 Hz, H$_{arom}$), 7.05 (t, 1H, *J*= 7.6 Hz, H$_{arom}$); ^{13}C NMR (213 MHz, DMSO-d_6) δ(ppm): 154.86, 154.81, 138.64, 137.38, 136.43, 135.25, 134.51, 134.27, 132.20, 130.85, 130.03, 128.80, 128.45, 128.41, 127.47, 126.48, 126.33, 126.26, 124.34, 122.68, 122.61, 120.04, 119.56, 118.06; Elem. Anal. for $C_{24}H_{17}Cl_2N_3O$: calcd C, 66.37; H, 3.95; Cl, 16.32; N, 9.68; O, 3.68; found C, 66.35; H, 3.97; Cl, 16.30; N, 9.66; O, 3.72.

Compound (5c): Light Yellow solid, yield: 80%; M.p.223-225°C; IR (cm^{-1}) *v*: 3321(OH), 3272 (NH), 1646(C=O), 1616(C=N), 1576(C=C); ^{1}H NMR (850 MHz, DMSO-d_6) δ(ppm): 12.15 (s, 1H, OH), 9.31 (s, 1H, NH), 8.95(s, 1H, NH), 8.65 (s, 1H, CH=N), 8.13 (d, 1H, *J*= 8.5 Hz, H$_{arom}$), 8.08 (dd, 1H, *J*= 8.5 Hz, *J*= 7.6,H$_{arom}$), 7.92 (m, 2H, H$_{arom}$), 7.81 (dd, 1H, *J*= 8.5, *J*= 7.6, Hz, H$_{arom}$), 7.67 (d, 1H, *J*= 8.5 Hz, H$_{arom}$), 7.58 (m, 1H, H$_{arom}$), 7.54 (t, 1H, *J*= 8.5 Hz, H$_{arom}$), 7.58 (t, 1H, *J*= 7.6 Hz, H$_{arom}$) 7.45 (m, 1H, H$_{arom}$), 7.29 (dd, 1H, *J*= 8.5,*J*= 7.6 Hz, H$_{arom}$), 7.27 (td, 1H, *J*= 8.5, *J*= 7.6 Hz, H$_{arom}$), 7.11 (td, 1H, *J*= 8.5,*J*= 7.6 Hz, H$_{arom}$), 7.01 (m, 2H, H$_{arom}$); ^{13}C NMR (213 MHz, DMSO-d_6) δ(ppm): 162.93, 160.16, 153.52, 139.87, 134.63, 134.22, 133.97, 133.74, 132.18, 128.84, 127.45, 127.04, 126.43, 126.32, 126.18, 123.92, 123.55, 122.30, 121.27, 120.83, 119.77, 119.28, 119.24, 117.05. Elem. Anal. for $C_{24}H_{19}N_3O_2$: calcd C, 75.57; H, 5.02; N, 11.02; O, 8.39; found C, 75.55; H, 5.05; N, 11.03; O, 8.37.

Compound (5d): Resynthesized and the experimental results are in agreement with ref(Aroua et al. 2022).

Compound (5e): Light yellow solid, yield: 86%; M.p. 249-250°C; IR (cm^{-1}) *v*: 3262(NH), 1644(C=O), 1624(C=N), 1590(C=C); ^{1}H NMR (850 MHz, DMSO-d_6) δ(ppm): 9.51 (s, 1H, NH), 8.78 (s, 1H), 8.74 (s, 1H), 8.27 (d, 1H, *J*= 7.6 Hz, H$_{arom}$), 8.16 (d, 1H, *J*= 8.5 Hz, H$_{arom}$),

7.98 (d, 1H, *J*= 8.5 Hz, H_{arom}), 7.95 (d, 1H, *J*= 7.6 Hz, H_{arom}), 7.93 (d, 1H, *J*= 7.6 Hz, H_{arom}), 7.86 (d, 1H, *J*= 7.6 Hz, H_{arom}), 7.78 (d, 2H, *J*= 8.5 Hz, H_{arom}), 7.72 (d, 1H, *J*= 8.5 Hz, H_{arom}), 7.60-7.47 (m, 5H, H_{arom}), 7.36 (d, 1H, *J*= 7.6 Hz, H_{arom}), 7.24 (t, 1H, *J*= 7.6 Hz, H_{arom}), 7.03 (t, 1H, *J*= 6.8 Hz, H_{arom}); ^{13}C NMR (213 MHz, DMSO-d_6) *δ*(ppm): 159.15, 154.14, 153.51, 138.51, 135.66, 135.15, 134.30, 132.32, 131.44, 128;90; 128.80, 127.86, 126.50., 126.34, 126.28, 126.11, 125.75, 124.43, 123.42, 122.68, 122.48, 119.38, 118.04, 117.83. Elem. Anal. for $C_{24}H_{18}BrN_3O$: calcd C, 64.88; H, 4.08; N, 9.46; O, 3.60; Br, 17.98; found C, 64.85; H, 4.11; N, 9.48; O, 3.60; Br, 17.96.

Synthesis of complexes 6a-c:

Resynthesized and the experimental results are in agreement with ref(Aroua et al. 2022).

An ethanolic solution of 1.5 mmol metals chloride salts of ($CrCl_3.6H_2O$, $CoCl_2.6H_2O$, and $CuCl_2.2H_2O$) in L:M molar ratios of 1:1 was added to a solution of urea-Schiff base (1.5 mmol) in 20 mL in ethanol. In the first 30 minutes the mixture of reaction was stirred at room temperature. After that, the mixture of reaction was stirred-refluxed for 3 hours. Thin Layer chromatography (Dimethylformamide/ethanol: 20/80) was used to monitor the reaction's progress. At the end of reaction, the mixture was cooled, filtered, and washed several times with hot absolute ethanol to remove non-reacting materials such as organic compound and metal salt materials, and after that dried under a vacuum.

***In vitro* antimicrobial activity**

The synthesized urea-Schiff bases and their metallic complexes were dissolved in DMSO at 10 mg/mL for the urea Schiff bases 5a, 5c, 5e, and 6b and 5mg/mL for urea Schiff base 5b, 5d, 6a, and 6c. For an antimicrobial test, all samples were sent to the Al-Thobhani medical laboratory. The investigated urea-Schiff bases and their metallic complexes were put to the test against pathogenic bacteria and fungus in *in vitro* biological screening experiments according to the disc diffusion method (Madani et al. 2022).*Staphylococcus aureus*, *Enterococcus faecalis* and *Staphylococcus aureus* negative-coagulase are examples of gram-positive bacteria. Gram-negative microorganisms include *Escherichia coli*; *Klebsiella pneumonia, Pseudomonas aerugenosa* as well as fungi, *Candida albicans* and *Aspergillus Niger*. According to clinical and laboratory standards, bacterial strains and fungal were carried out and uniformly spread with swabs on petri plates containing Agar in order to screen the antibacterial activity and antifungal activity of urea-Schiff base and its metal complexes of analogs. The investigated substances were applied on paper disks (Labor CLIN) at a concentration of 5 mg/L after being dissolved in DMSO (Sigma-Aldrich) 99.9%. The results were clarified by measuring the inhibition zone (mm) that formed around the disk after the incubation period at 37 °C between 18 and 24 hours. DMSO served as the employed negative control. Both Erythromycin (for Gram-positive bacteria) and ciprofloxacin (for Gram-negative strains) were used as positive controls. Three separate triplicates were used for the assays.

Minimum inhibitory concentration

For the urea-Schiff base cobalt complex (6b), which was the active molecule found through the disk diffusion method, the Minimum Inhibitory Concentration (MIC) was evaluated using the dilution method. The MIC is the lowest level of (6b) that inhibits Gram-positive bacterial growth that is observable. In a 96-well microplate, the 6b was diluted in 100 µL of liquid growth media at concentrations ranging from 0.079 to 2.5 µg/mL (0.079, 0.157, 0.313, 0.625, 1.25, and 2.5 µg/mL). Then, 100 µL of a suspension of Gram-positive bacteria was added to each well, along with an inoculum comprising 106 CFU (colony forming units)/mL. The system's greatest DMSO concentration, 5%, had no impact on the development of any microorganisms. Gram-positive bacteria were tested using erythromycin as a positive control. The existence of turbidity or silt after 24 hours of incubation at 37°C shows the development of microorganisms, and the MIC was established by the lower concentration that produced no turbidity (Madani et al. 2022).The experiments were carried out three times.

Molecular Docking

Schiff base derivatives of urea 5a-e and their complexes 6a-cinteracts with *S. aureus* tyrosyl-tRNA synthetase and is investigated using molecular docking to explain the preferred arrangement of the ligands in the receptor's active region. The enzyme model's crystal structure was taken from the Protein Data Bank: *S. aureus* tyrosyl-tRNA synthetase (PDB code 1JIJ). The models are created without the use of any H_2O molecules or the co-crystallized ligand. To incorporate Gasteiger charges and Polar hydrogens, AutoDock Tools1.5.2 (ADT) was utilized, and the file type PDBQT was developed (Morris et al. 2008). Using ADT, we chose the grid for docking. In 1JIJ, the grid box was centered at x:10.908, y: 14.432 and z: 86.420. The coordinates x, y, and z for the grid box size were 25 with a spacing of 0.375. The geometry of the urea Schiff base derivatives 5a-e and their complexes 6a-cin Gaussian G09 (Frisch et al. 2013)has been refined using the PM6 approach. The PDB file was converted to the PDBQT format using ADT. To execute the docking simulations, we used Auto Dock Vina software (Trott et al. 2010)with an exhaustiveness setting of 32. ADT was used to investigate the docking conformations. For examining ligand-receptor interactions, the Discovery Studio Visualizer was employed (Dassault Systems2010).

RESULTS AND DISCUSSION

Chemistry

O-Phenylenediamine 1 and 1-naphthyl isocyanate 2 were first condensed in equimolar proportions under

catalyst-free in anhydrous dichloromethane to produce amino-urea 3 (scheme 1). In the second step, arylaldehydes 4 was used to convert the obtained amino-urea 3 into Schiff base-ureas5a-e(scheme 1) under reflux following the literature conditions (Aroua et al. 2022).

The targeted complexes 6a-c have been synthesized in L:M ratios of 1:1 (Scheme 2) by treating an ethanol solution of the ligand HL (5d) with metal chloride salts ($CuCl_2.2H_2O$, $CoCl_3.6H_2O$,$CrCl_3.6H_2O$) according the literature condition (Aroua et al. 2022).

FT-IR, UV-Vis, CHN, TGA-DTA, XRD powder and SEM were used for analyzing the target metal complexes as well as conductivity and magnetic moment susceptibility tests. Table 1 summarizes the analytical data of ligand 5d and complexes 6a-c.

^{1}H and ^{13}C NMR spectra of compounds 5a-e

Spectroscopic methods were used to determine the structures of new synthesized substances 5a-e. FT-IR, ^{1}H NMR, ^{13}C NMR, and elemental analysis are some of the techniques used. The infrared spectra of target 5a-e showed the following distinctive bands including NH group in the range of 3286 to 3262, carbonyl group CO in the range of 1648 to 1629, CN motif in the range of 1624 to 1553 and C=C band appear in the range of 1590 to 1532 cm^{-1}. ^{1}H NMR of compounds 5a-erevealed two singlets in the range of 9.52 to 9.32 and 9.22 to 8.74 ppm, attributed to the NHs of the urea moieties. Azomethine proton resonated as a singlet in the range of δ_H 8.76 to 8.54ppm. In the aromatic common region range δ_H 8.28 to 7.01 ppm the aromatic protons were identified. Downfield singlets of hydroxyl groups were observed at 12.15 and 15.12 ppm for products 5c and 5d, respectively.

^{13}C NMR spectra of compounds 5a-eindicated a singlet attributed to C=O of the urea moiety in the range of 154.86 to 153.51 ppm. Another singlet corresponding to the azomethine carbon appear in the range of 160.16 to 158.9 ppm. The remaining carbons of aromatic rings were found in normal aromatic area, ranging from 153.7 to 110.1 ppm. Carbons with attached hydroxyl group resonate as a singlet at 162.93 and 167.10 ppm for compounds 5c and5d, respectively.

The FT-IR spectra of ligand 5d, for example, revealed the following particular bands: 3274, 3262 cm^{-1} for NHs, 1646 cm^{-1} corresponding to carbonyl group, 1616 cm^{-1} attributed to azomethine group, and 1576 cm^{-1} relatively to double bond (C=C). ^{1}H NMR spectrum revealed a downfield singlet at 15.12 ppm attributed to hydroxyl proton. The spectra of targeted compound 5d indicated two singlets centered at 9.69 and 9.22 ppm attributed to proton of urea moiety. The proton of the azomethine group displayed a doublet at 8.73 ppm. The other aromatic protons appeared in the aromatic protons common region at δ_H ranging 8.28 to 7.01 ppm. Spectraof ^{13}C NMR for ligand 5d present a singlet at 167.1 ppm attributed to phenolic carbon and another singlet at 153.74 ppm identified to carbonyl group of urea moiety. The proton of azomethine group centered at 158.9 ppm. Other carbons of aromatic rings resonated in the common aromatic region around 138.7 to 110.1 ppm.

Measurements of molar conductivity

The complex's molar conductance values showed low values in DMF solvent (10^{-3}M) varying from 14.7 to 28.2 cm^2 mol^{-1}. this value indicates that the metal complexes are non-ionic (Table 1).According to Al-Hakimi et al. (Al-Hakimi et al. 2011), El-Saied et al. (El-saied et al. 2020), and El-Tabl et al(El-Tabl et al. 2012).

Susceptibility of magnetic moments

The magnetic susceptibility of the metal complexes at room temperature were listed in (Table 1). The result indicated that the copper (II) complex 6a manifested a value of 1.78 B.M. presenting a distorted octahedral geometry around the Cu(II) ion. While the magnetic susceptibility value of the cobalt (III) complex showed 4.2 B.M. This value indicates a high spin octahedral shape around the cobalt (III) ions. The metal complex of Chromium (III), showed the magnetic susceptibility measurement was 1.82 B.M. This low value implies that the Cr(III) ion has an extremely low spin octahedral structure.

Infrared spectra

Infrared spectroscopy is an essential tool to specifying the functional moieties in studying chemical compounds. Furthermore, this approach identifies the bonding locations in complexes between the metal ions and the ligands, that were examined. In the actual investigation, ligand HL demonstrated multitude vibrations demonstrating the presence of functional groups. The ligand exhibited two vibration bands emerged at 3274 cm^{-1} and 3264 cm^{-1}, suggesting (NH) group vibrations, whereas carbonyl group (C=O) vibrations manifested at 1647 cm^{-1}. The imine group was detected at 1616 cm^{-1}, (C=C) bond was revealed at 1576 cm^{-1}. Phenolic hydroxyl group vibrations were absent in the IR spectra (Table 2) however this band was detected in ^{1}H NMR spectra at 15.12 ppm.

The behavior of urea-Schiff base HL in their complexes indicated monobasic bidentate in complex (6c), in interaction with HL linked to the metal via the phenolic OH group and the azomethine group via nitrogen (C=N) (Table 2). The absence of the bands corresponding to hydroxyl group v(OH) in all compounds is an indicative to verified this bonding tendency. The behavior of ligand, is neutral bidentate, showed in complexes (6a) and (6b), where HLit was bonded to metal ions via the oxygen atom of hydroxyl motif and the imine group via nitrogen.

In the other hand, complexes manifested in the range of 3265 to 3600 cm^{-1} a wide band, indicating the existence of water molecules, while hydroxyl group linked with metal ion manifesting a sharp or medium band at 3480 and 3450 cm^{-1}, respectively. It also reported a change in the azomethine group's vibrational bands in a range of 1595 to 1611 cm^{-1}, this value indicated the bonds of metal with the nitrogen atom. According to Al-Hakimi (Al-Hakimi et al.

2020), Shakdofa et al. (Shakdofaet al. 2021), and T. Alorini et al. (Alorini et al. 2023), on the other hand, complexes displayed also a band in the range of 631 to 695, 520 to 567, and 401 to 410 cm^{-1}, which indicated respectively the vibrations of (M-O), (M-N), and (M-Cl).

3.1.5. UV-Vis spectra

The absorption bands exhibited by the ligand HL (5d) at 221, 301, and 391 nm refer to the nonbonding electrons transitions on both nitrogen and oxygen atoms manifesting electronic transitions $n\rightarrow\pi^*$, $\pi\rightarrow\pi^*$ and $\sigma\rightarrow\sigma^*$ respectively (Table 3). While these transitions in metal complexes shifted and they appeared indicating a distinctive d-d transitions.

The copper (II) complex (6a) showed two electronic bands at 500 and 390 nm (Table 3). corresponding to $2B_1\rightarrow 2E$ and $2B_1\rightarrow 2B_2$ transitions around the Cu(II) ion in deformed octahedral shape.

The cobalt (III) complex (6b) showed also two important electronic bands at 520 and 380 nm attributed to $4T_{1g}$ (F)$\rightarrow$ $4T_{1g}$(P) and $4T_{1g}$(F)$\rightarrow 4A_{2g}$ transitions respectively, identical to octahedral shape around cobalt (II) ion. Some researchers published Al-Hakimi and co-workers (Al-Hakimi et al. 2011), El-Tabl and collaborators (El-Tabl et al. 2012), Shakdofaand colleagues (Shakdofa et al. 2021) indicating that metal complexes displayed distinct electronic bands due to Ligand-Metal Charge Transfer (LMCT) transition or signaling intra-ligand absorption corresponding to the complex (6c).

Thermal analysis

To ascertain the thermal stability of metal complexes, a thermal analysis was performed. The TG-DTA curves of Cu-, Co-, and Cr- complexes were recorded in a range of temperature from 25 to 500°C and given in Figure 1. The thermogravimetric analysis (TGA) curves show that the complexes are stable. Some complexes TGA findings matched the elemental analysis formula. According to TGA data, the complexes were destroyed sequentially (El-Tabl et al. 2012,Shakdofaet al. 2021,Buldurun et al. 2021,Al-Hakimi et al. 2021).

The Cu(II) and Cr(III) complexes showed four steps of decomposition. at 60–90°C first step occurred with losses of 5.96 and 9.20 % (calcd. 5.98 and 9.16 %) respectively due to the elimination molecules of water (Table 4). In the range of 130–150 °C, second step take place with weight losses of 5.95 and 6.10% (calcd. 5.98 and 6.11%) respectively indicating the exclusion of water molecules. Third stage occurs in the range of 230 to 250 °C with loss of 6.10 and 12.23 % weight (calcd 6.06 and 12.20 %) respectively corresponding to elimination of hydrochloride molecules from complexes. Last stage performed in the range of (400 to 500) and (420 to 500) °C with losses weight of 68.60 and 46.54 % (calcd. 68.78 and 64.89%) respectively indicating the full decomposition of complexes and transformed to metal oxides 13.21 and 25.77 % for (CuO, and Cr_2O_3), respectively.

The Co(III) complex decay in three temperature steps. the first step occurred between the range 130–150 ^oC, with a loss of 6.09 (calc. 6.02) by weight corresponding to removal molecules of water (Table 4).

While the second step exhibited a temperature range of 230 to 250 °C with losses of 11.84 % by weight (calcd. 11.88 %), due to the elimination of the hydrochloride molecule.

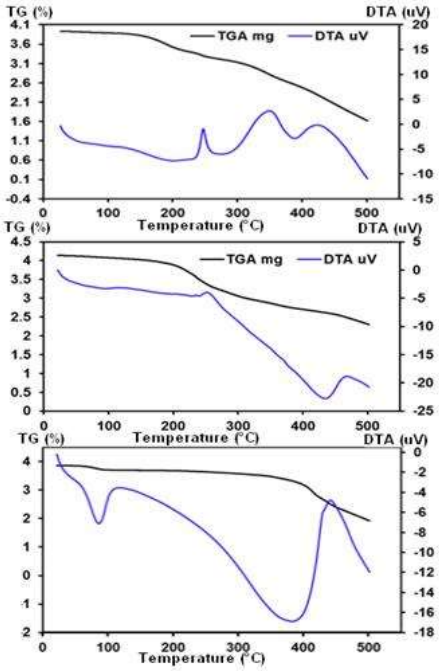

Figure 1: Thermal analyses (TG/DTA) of (a) Cu(II), (b) Co(II), and (c) Cr(III) complexes.

On the other hand, the third step happened between 450- 500 °C range with losses of 60.13 % by weight (calcd. 60.11 %) due to the complex decay and transformation to metal oxide 27.80 % (calcd. 27.76 %) corresponding to Co_2O_3(Al-Hakimi et al. 2021, Alorini et al. 2022).

XRD analysis

A Rigaku XRD diffractometer (Ultima IV, USA) using CuKα radiation (λ= 1.54056 Å) conducted at 40 kV and 30 mA, X-ray diffraction patterns (XRD) of the produced complexes compounds were elaborated. Fullprof software (Rietveld et al. 1969)was applied to the Rietveld refinement method. The obtained XRD patterns of the ligand and Co-, Cu-, and Cr complexes were recorded in Figure 2.

As shown in figure 2, Cr-complex has an amorphous structure. The crystal data and the unit cell parameters are listed in Table 5. As shown, the ligand HL has monoclinic crystal structures with space group P1211, while the Co and Cu complexes have triclinic and tetragonal crystal structures with space groups P-1 and P4/nmm, respectively.

Moreover, from the main XRD peaks, the average crystallite size of the as-prepared complexes can be quantified by using the Debye-Scherrer equation below:

$$D = \frac{K\,\lambda}{\beta \cos\theta}$$

where β is the full width at half-maximum of the diffraction peak, θ is the Bragg angle, λ (0.15406 nm) is the wavelength of the X-ray, D is the crystallite size and K is a dimensionless shape factor (K=0.9). The values of crystallite sizes, D, are also listed in Table 5.

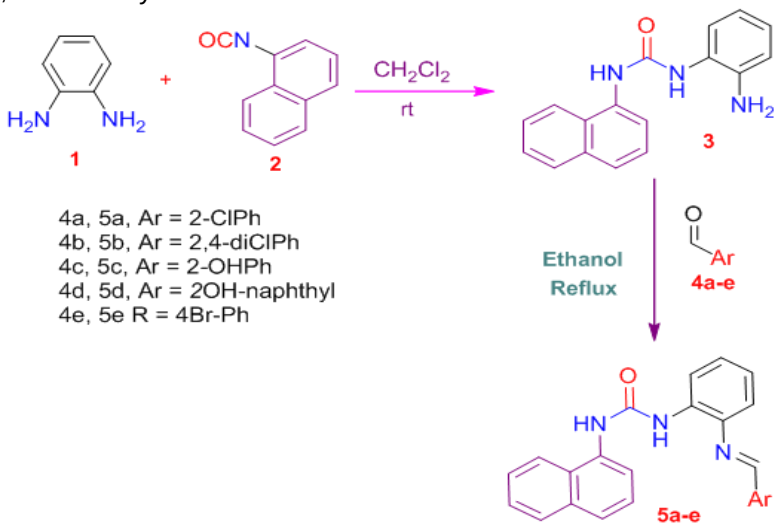

Scheme 1: Synthesis of urea-Schiff bases 5a-e

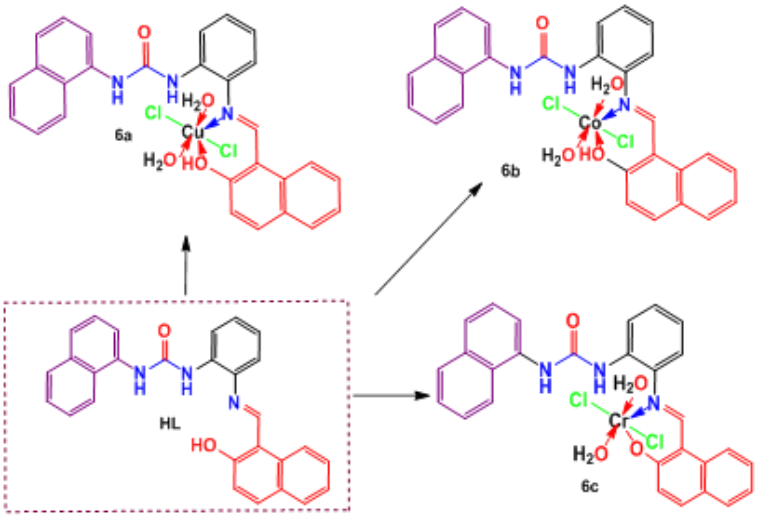

Scheme 2: Urea Schiff base complexes synthesized

Table 1: Some analytical characteristics and physical for the urea Schiff base ligand and its metal complexes.

Compound	Colour	M.Wt.	Calcd (Found) %			M	Λ^a	(%) of
			C	H	N			Yield
HL ($C_{28}H_{21}N_3O_2$)	Light Yellow	431.50	77.94(77.92)	4.91(4.89)	9.74(9.72)	---	-----	80
$C_{28}H_{25}Cl_2CuN_3O_4$	Red	601.97	55.87 (55.86)	4.19(4.16)	6.98(6.95)	1.78	20.3	85
$C_{28}H_{25}Cl_2CoN_3O_4$	Red	597.36	56.30 (56.29)	4.22(4.21)	7.03(7.01)	4.2	14.7	78
$C_{28}H_{25}Cl_2CrN_3O_4$	Red	589.41	57.06 (57.03)	4.10(4.08)	7.13(7.11)	1.82	28.2	70

: Molar conductivity unit $^a\Lambda$ (Ω^{-1} cm^2 mol^{-1}),M: Magnetic moments susceptibility (B.M.)

Table 2: IR spectra ligand and its metal complexes

Comp	v (OH)	v(H_2O) Coord).	v (NH)	v (C=O)	v(C=N)	v(C=C)$_{Ar}$	v(M-O)	v(M-N)	v(M-Cl)
HL	-------	------	3274, 3264	1646	1616	1576	------	------	-----
Cu	-------	3660-3270	3272,3260	1650	1619	1597	691	527	410
Co	3260-2980	3650-3265	3268,3263	1647	1620	1593	694	520	405
Cr	-------	---------	3270,3262	1650	1616	1592	695, 656	617	409

Table 3: The electronic transition of the studied compounds in ethanol

No.	Ligand / Complexes	λ_{max} (ethanol)	ε (mol^{-1} cm^{-1})
5d	HL ($C_{28}H_{21}N_3O_2$)	391, 301, 221	7.9 X10^{-3}, 5.2 X10^{-3}
6a	$C_{28}H_{25}Cl_2CuN_3O_4$	501, 381, 332, 312, 262	1.7 X10^{-4}, 3.2 X10^{-4}, 1.2 X10^{-3}
6b	$C_{28}H_{25}Cl_2CoN_3O_4$	473, 319, 312, 257	3.4 X10^{-4}, 3.0 X10^{-4}, 1.4 X10^{-3}
6c	$C_{28}H_{24}Cl_2CrN_3O_4$	452, 373, 257	5.7 X10^{-3}, 4.1 X10^{-4}, 4.1 X10^{-3}

Table 4: Thermal analysis of metal complexes

M-complex	Loss coordinated Water % at (130-150) ^{0}C Calcd.(found)	Loss chloride % at (230- 250) ^{0}C Calcd.(found)	% of the remaining portionat (550- 650) ^{0}C Calcd. (found)
Cu-	5.98 (5.96) ($2H_2O$)	6.06 (6.10) (HCl)	13.21 (13.11) (CuO)
Co-	6.02 (6.09) ($2H_2O$)	11.88 (11.84) (2HCl)	27.80 (27.76) (Co_2O_3)
Cr-	6.11 (6.10) ($2H_2O$)	12.20 (12.23) (2HCl)	25.77 (25.77) (Cr_2O_3)

Table 5: XRD data of ligand and Co- and Cu- complexes

Parameters		HL (1)	Co-complex	Cu-complex
Lattice constant	a (Å)	12.32(1)	11.62 (1)	17.68(1)
	b (Å)	23.41(1)	11.53(1)	17.68(1)
	c (Å)	11.01(1)	10.04(2)	10.41(1)
Inter axial angle	α (°)	90.00	115.6(13)	90.00
	β (°)	90.1	104.0(19)	90.00
	γ (°)	90.00	73.4(16)	90.00
Crystal system		Monoclinic	Triclinic	tetragonal
Space group		$P2_1$	*P-1*	*P4/nmm*
Unit cell Volume (Å^3)		3175	1151	3254
Crystallite size, D (nm)		15	20	35
Agreement factors, Rb (%) Rwp(%) GOF		3.11 3.74 1.20	2.52 2.69 1.06	2.55 2.85 1.11

Table 6: Inhibition zones (mm) of bacterial growth induced by urea-Schiff base and its metal complexes.

Tested substance	Gram-positive bacteria			Gram-negative bacteria			*Fungi*	
	***S. aureus* CP**	***S. aureus* CN**	***E. faecalis***	***E.* coli**	***K. pneumonia***	***P. aerugenosa***	***C.* albicans**	***A. Niger***
5a (10 µg/mL)	-	-	-	-	-	-	-	-
5b (5 µg/mL)	-	-	-	-	-	-	-	-
5c(10µg/mL)	-	-	-	-	-	-	-	-
5d (5 µg/mL)	-	-	-	-	-	-	-	-
5e (10 µg/mL)	-	-	-	-	-	-	-	-
6a (5 µg/mL)	-	-	-	-	-	-	-	-
6b(10 µg/mL)	17 ± 3	13 ± 2	14 ± 2	-	-	-	-	-
6c (5 µg/mL)	-	-	-	-	-	-	-	-
DMSO (5%)	-	-	-	-	-	-	-	-
Ciprofloxacin				24 ± 3	23 ± 3	22±5		
Erythromicin	22 ± 2	20 ± 2	23 ± 3					
Econazol							28 ± 2	27± 3

SS. aureus CP =Staphylococcus aureus coagulase positive; S. aureus CN= Staphylococcus aureus coagulase negative; Enterococcus faecalis,E.coli, K. pneumonia= Klebsiella pneumonia;Pseudomonas aerugenosa, C. albicans= Candida albicans and Aspergillus Niger. Note: Each test was performed in triplicate. All the results are expressed in mean ± SD. - : compound with low or did not show any

activity.

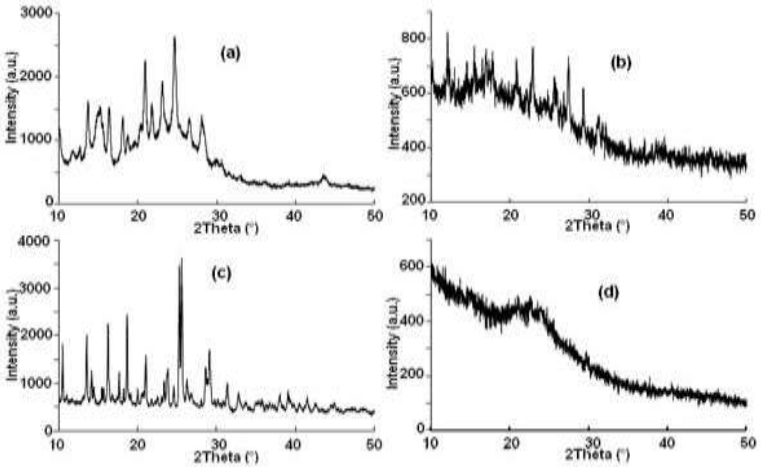

Figure 2: XRD patterns of the ligand (HL) (a), Co-complex (b), Cu-complex (c), and Cr-complex (d).

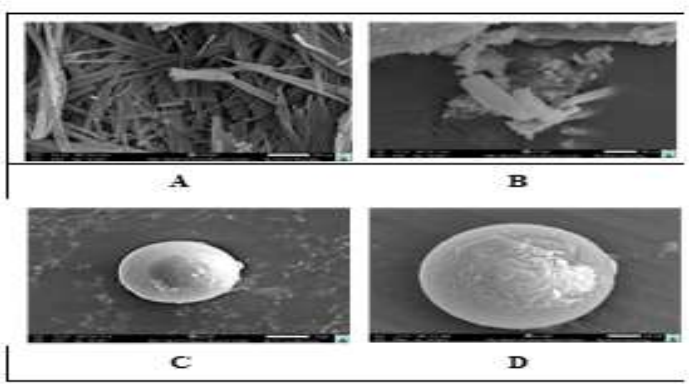

Figure 3: SEM image of products: A: ligand HL, B: Cobalt complex, C: Chromium complex, D: Copper Complex.

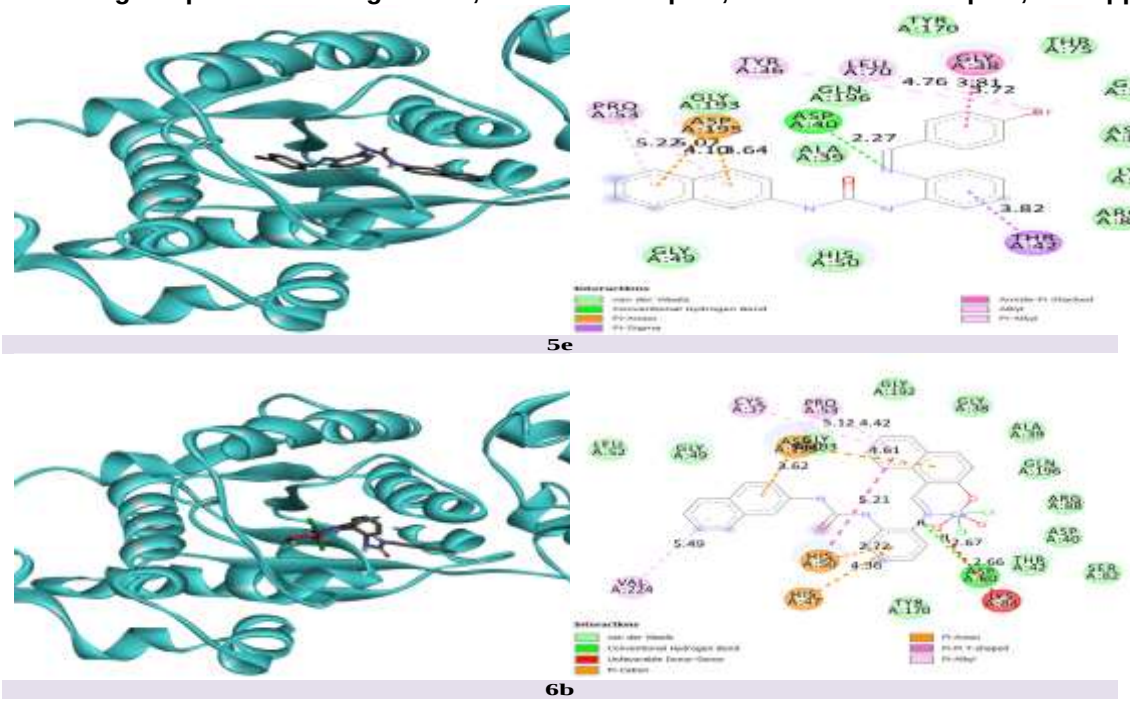

Figure 4: Three dimensional structures (3D) and two-dimensional interactions (2D) of 5e and 6b with the amino acids of the catalytic site of tyrosyl tRNA-synthetase (PDB: 1JIJ).

We note that the broadening of XRD pattern peaks indicates that the crystallites are in the order of nanometre size. As shown in Table 5, the crystallite size of these complexes varies from 15 to 35 nm.

SEM analysis

Figure 3 gives typical SEM-images of the compounds which they revealed a variety of forms. As shown, the ligand HL carried on a sticky structure (Fig. 3A), whereas cobalt (II) complex present a random shape (Fig. 3B), copper and chromium complexes adopted a spherical shape (Fig. 3C and 3D) (Alorini et al. 2022).

Antimicrobial activity

The pathogenic bacteria *Staphylococcus aureus*, *Enterococcus faecalis*, *Staphylococcus aureus* coagulase-negative, *Escherichia coli*, *Klebsiella pneumonia*,*Pseudomonas aerugenosa*and fungi (*Candida albicans,Aspergillus. Niger*) were used in tests on the urea Schiff bases and its metal complexes in the microbiology lab. Except for cobalt complex (6b) (10 µg/mL), which showed a clear and distinct action against the pathogenic bacteria, none of the substances showed any antibacterial impact against the bacteria strains (Table 6). The compound 6b has demonstrated better antibacterial action against the tested Gram-positive bacteria *Staphylococcus aureus* (CP), *Enterococcus* and *Staphylococcus aureus* (CN) respectively (17±3, 14±2 and 13±2 mm) than the other urea Schiff base and its metal complexes, is comparable to that of the reference antibiotic.

All of the urea-Schiff bases and complexes failed the antibacterial and the antifungal activity screen tests when tested against the Gram-negative bacteria and against *Candida albicans* and*Aspergillus Niger*. The urea-Schiff base cobalt complex (6b), shown in Table 6, exhibits antimicrobial activity against Gram-positive bacteria, but not against Gram-negative bacteria and fungi as well. The Minimum Inhibitory Concentration MIC of complex 6b was 2.5 µg/mL. This result is comparable to reference drug erythromycin (MIC: 3 µg/mL). The unique characteristics of the antimicrobial drugs and the target microorganisms can be used to explain the differences in antimicrobial activity against bacteria and fungi.

Numerous research works have looked into the characteristics of the antibacterial actions of urea-Schiff bases cobalt complex. It has been revealed that cobalt complex with Schiff base ligands made from different amino acids and salicylaldehyde have demonstrated antibacterial properties (Saghatforoush et al. 2009).

Comparing the antimicrobial activity of the cobalt complex Schiff base-urea on a variety of bacterial strains, including *Staphylococcus aureus* (Gram-positive), *Escherichia coli* (Gram-negative), and *C. albicans*, allowed researchers to assess the cobalt complex's antibacterial potential (Shaygan et al. 2018, Rezaei et al. 2023, Kumari et al. 2019, Gurubilli et al. 2023).

This 6b behavior in the target microorganisms can be explained by a number of factors. One possibility is 6b target a component of bacterial cells that is not present in *C. albicans*. The bacterial cell wall composed of peptidoglycan, a unique molecule not found in fungal cell walls structure, this urea-Schiff bases Co-complex is not effective against it. Another possibility is that the urea-Schiff bases Co-complex may be unable to penetrate the cell wall of Gram-negative bacteria and *C. albicans*. Fungal cell walls are composed of different molecules, such as chitin and glucans, which may be more resistant to urea-Schiff bases Co-complex than Game-positive bacterial cell walls. Lastly, it's possible that the urea-Schiff bases Co-complex may have different mechanisms of action against bacterial and fungal cells. For example, some substances may target bacterial-specific enzymes or metabolic pathways, while others may have more specific targets in cells.

***In silico* Docking Study**

Binding energies:

For the compounds 5a-e and 6a-c, we used molecular docking. To investigate the binding mode of the compounds, the catalytic domain of Tyr RS from S. aureus was studied.Tyrosyl-tRNA syntheses, which plays a crucial role in protein creation, has been shown to be one of the most important targets of antimicrobial drugs in the fight against drug-resistant bacteria (Othman et al. 2021).

Table 7: Binding energies of 5a-e and6a-c with TyrRS receptor (PDB: 1JIJ).

Compound	Free binding energy (kcal mol^{-1})
5a	-10.4
5b	-10.4
5c	-10.2
5d	-11.7
5e	-10.1
6a	-9.9
6b	-8.9
6c	-9.3

We investigated their affinity and interactions with key residues. Table 7 summarizes the findings. The docking investigation of molecules 5a-e and 6a-c revealed binding energy values ranging from 8.9 to 11.7 kcal/mol.

When comparing the binding energies in our study, which range from -8.9 to -10.4 kcal/mol, with those of other systems docked to the same protein as reported in reference (Othman et al. 2021)(binding energies ranging from -6.01 to -7.58 kcal/mol), we observe that our interaction energies are more favorable. Furthermore, in reference (Rugaie et al. 2023), which investigates other systems with the same protein and reports binding energies ranging from -6.2 to -10.1 kcal/mol, some of their molecules exhibit energy ranges similar to ours.

Analysis of Receptor-ligands interaction:

Figure 4 displays the interactions produced by the

designated ligands and the active site of Tyr RS using a *S. aureus* simulation built from the Tyr RS complex structure (pdb code: 1jij). The ligands 5e and complex 6b were selected from the most active compounds in the antibacterial experiments. The docking study aims to provide insight into the potential antibacterial action of these compounds.

5e interactions

The binding energy of 5e is -10.1 kcal mol^{-1}. It forms a single hydrogen bond with Asp40. There are two interactions between π-anion and Asp195. It has four alkyl connections with Leu70, Tyr36, and Pro53 (2 interactions), and it fits in extremely well with several Van der Waals contacts in the active site.

6b interactions:

6bhas a binding energy of -8.9 kcal mol^{-1}. With Asp80, it forms one hydrogen bond. There are two π-alkyl interactions with Pro53 and one with Cys37. π-ion interactions with Asp195 (two interactions), His50, and His47 present four connections. VdW interactions surround the molecule with many amino acids.

The various results demonstrate that 5e and 6b have a high affinity for the enzyme active site and interact with the key residues. This implies that these findings contribute to antibacterial activity. Our findings concerning interactions with Gly38, Leu70, Thr75, Tyr170, Asp40, and Cys37 are consistent with those reported by Beg et al. (Beg et al. 2020).

CONCLUSION

A Schiff base-urea derivatives 5a-e were synthesized via the condensation of *o*-phenylenediamine, 1-naphthyl isocyanate, and a suitable aryl aldehyde. Cu^{2+}, Co^{2+}, and Cr^{3+} were employed to elaborate new mononuclear complexes 6a-c from a hybrid urea Schiff base HL (5d). The results reveal that the ligand HL interacts with metal ions as a monobasic or neutral monodentate chelator in an octahedral shape employing azomethine nitrogen and a deprotonated/protonated phenolic oxygen atom. The elemental analysis of the complexes indicated that in all-metal complexes, the ligand binds with the metal ions in a 1:1 ratio. The ligand and its complexes adopted monoclinic, tetragonal, and orthorhombic structures, which correspond to Schiff base-urea HL, cobalt complex (6b), and copper complex (6a). The Schiff base-urea derivatives 5a-e and complexes 6a-c were tested for antimicrobial activities. Cobalt complex (6b) demonstrated a strong antibacterial activity against gram positive bacteria *Staphylococcus aureus* (CP), *Enterococcus faecalis* and *Staphylococcus aureus* (CN) respectively (17 ± 3, 14 ± 2 and 13 ± 2 mm) comparable to standard reference drug Erythromycin. The minimum inhibitory concentration of cobalt complex was also determined MIC value found 2.5 µg/mL similar to the standard reference drug Erythromycin.

Funding statement

This study was supported byQassim University, represented by the Deanship of Scientific Research, on the financial support for this research under the number (10190-cos-2020-1-3-I) during the academic year 1442 AH / 2020 AD.

Institutional Review Board Statement

The study was approved by the Bioethical Committee of the Qassim University Health Research Ethics Committee

Informed Consent Statement

Not applicable.

Data Availability Statement

All of the data is included in the article/Supplementary Material.

Acknowledgments

The authors gratefully acknowledge Qassim University, represented by the Deanship of Scientific Research, on the financial support for this research under the number (10190-cos-2020-1-3-I) during the academic year 1442 AH / 2020 AD.

.

AUTHOR CONTRIBUTIONS

Conceptualization, L.M.A. and A.N.H.; methodology, L.M. A., A.N.H., M.A. M.A; software, L.M. A., A.N.H., M.A.M.A.; validation, L.M.A., A.N.H., M.A.M.A; formal analysis, L.M.A., A.N.H., M.A.M.A, S.K.H.; investigation, L.M.A., A.N.H., M.A.M.A.; data curation, L.M.A., A.N.H., M.A.M.A.; writing-original draft preparation, L.M.A., A.N.H.; writing-review and editing, L.M.A., A.N.A., M.A.M.A.; visualization, L.M.A., A.N.H.; funding acquisition, L.M.A., All authors have read and agreed to the published version of the manuscript.

Conflict of interest

The authors declared that present study was performed in absence of any conflict of interest.

Peer Review: ISISnet follows double blind peer review policy and thanks the anonymous reviewer(s) for their contribution to the peer review of this article.

REFERENCES

Abu-Yamin, A.A., Abduh, M.S., Saghir, S.A.M. and Al-Gabri, N., 2022. Synthesis, characterization and biological activities of new Schiff base compound and its lanthanide complexes. Pharmaceuticals, 15(4), p.454.

Alhakimi, A.N., 2020. Synthesis, Characterization and Microbicides Activities of N-(hydroxy-4-((4-nitrophenyl) diazenyl) benzylidene)-2-(phenylamino) Acetohydrazide Metal Complexes. Egyptian Journal of Chemistry, 63(4), pp.1509-1525.

Al-Hakimi, A.N., Shakdofa, M.M., El-Seidy, A. and El-Tabl, A.S., 2011. Synthesis, Spectroscopic, and Biological Studies of Chromium (III), Manganese (II), Iron (III), Cobalt (II), Nickel (II), Copper (II), Ruthenium (III), and Zirconyl (II) Complexes of N 1, N 2-Bis (3-((3-hydroxynaphthalen-2-yl) methylene-amino) propyl) phthalamide.Journal of the Korean Chemical Society, 55(3), pp.418-429.

Al-Hakimi, A.N., Shakdofa, M.M., Saeed, S., Shakdofa, A.M., AlFakeh, M.S., Abdu, A.M., Alhagri, I.A., 2021. Transition Metal Complexes Derived from 2-hydroxy-4-(p-tolyldiazenyl) benzylidene)-2-(p-tolylamino) acetohydrazide Synthesis, Structural Characterization, and Biological Activities. J. Korean Chem. Soc. 65 (2), 93–105.

Alminderej, F.M. and Lotfi, A., 2021.Design, Synthesis, Characterization and Anticancer Evaluation of Novel Mixed Complexes Derived from 2-(1H-Benzimizadol-2-yl) aniline Schiff base and 2-Mercaptobenzimidazole or 2-Aminobenzothiazole. Egyptian Journal of Chemistry, 64(7), pp.3351-3364.

Alorini, T., Al-Hakimi, A.N., Daoud, I., Alminderej, F., Albadri, A.E. and Aroua, L., 2023. Synthesis, characterization, anticancer activity and molecular docking of metal complexes bearing a new Schiff base ligand. Journal of Biomolecular Structure and Dynamics, pp.1-16.

Alorini, T.A., Al-Hakimi, A.N., Saeed, S.E.S., Alhamzi, E.H.L. and Albadri, A.E., 2022. Synthesis, characterization, and anticancer activity of some metal complexes with a new Schiff base ligand. Arabian Journal of Chemistry, 15(2), p.103559.

Amirthaganesan, K., Vadivel, T., Dhamodaran, M. and Chandraboss, V.L., 2022. In vitro antifungal studies of ruthenium (III) complex derived from chitosan Schiff bases. Materials Today: Proceedings, 60, pp.1716-1720.

Aroua, L., 2020. Novel Mixed Complexes Derived from Benzoimidazolphenylethanamine and 4-(Benzoimidazol-2-yl) aniline: Synthesis, characterization, antibacterial evaluation and theoretical prediction of toxicity. Asian Journal of Chemistry, 32(6), pp.1266-1272.

Aroua, L.M., Alhag, S.K., Al-Shuraym, L.A., Messaoudi, S., Mahyoub, J.A., Alfaifi, M.Y. and Al-Otaibi, W.M., 2023. Synthesis and characterization of different complexes derived from Schiff base and evaluation as a potential anticancer, antimicrobial, and insecticide agent. Saudi Journal of Biological Sciences, 30(3), p.103598.

Aroua, L.M., Al-Hakimi, A.N., Abdulghani, M.A. and Alhag, S.K.,2022. Elaboration of novel urea bearing schiff bases as potent in vitro anticancer candidates with low in vivo acute oral toxicity. Main Group Chemistry, 21, 953–973.

Aroua, L.M., Al-Hakimi, A.N., Abdulghani, M.A. and Alhag, S.K.,2022. Elaboration of novel urea bearing schiff bases as potent in vitro anticancer candidates with low in vivo acute oral toxicity. Main Group Chemistry, 21, 953–973.

Beg, M.A.; Ansari, S.; Athar, F. 2020. Molecular docking studies of Calotropis gigantea phytoconstituents against Staphylococcus aureus tyrosyl-tRNA synthetase protein. J. Bacteriol. Mycol., 8, 78–91.

BhagwatraoBiradar, S.; VithalNarte, D.; Pradip Kale, R.; Momin, K.I.; Sudewad, M.S.; Tayade, K.C.; Palke, D.G. Synthesis, spectral and biological studies of DHA Schiff bases. *J.* Appl. Organometal. Chem. 2021, 1, 41–47.

Borrego-Muñoz, P., Becerra, L.D., Ospina, F., Coy-Barrera, E. and Quiroga, D., 2022. Synthesis (Z) vs (E) selectivity, antifungal activity against Fusarium oxysporum, and structure-based virtual screening of novel Schiff bases derived from L-tryptophan. ACS omega, 7(28), pp.24714-24726.

Borrego-Muñoz, P., Cardenas, D., Ospina, F., Coy-Barrera, E. and Quiroga, D., 2023. Second-Generation Enamine-Type Schiff Bases as 2-Amino Acid-Derived Antifungals against Fusarium oxysporum: Microwave-Assisted Synthesis, In Vitro Activity, 3D-QSAR, and In Vivo Effect. Journal of Fungi, 9(1), p.113.

Buldurun, K., Turan, N., Bursal, E., Aras, A., Mantarcı, A., Çolak, N., Türkan, F. and Gülçin, İ., 2021. Synthesis, characterization, powder X-ray diffraction analysis, thermal stability, antioxidant properties and enzyme inhibitions of M (II)-Schiff base ligand complexes. Journal of Biomolecular Structure and Dynamics, 39(17), pp.6480-6487.

Canale, V., Czekajewska, J., Klesiewicz, K., Papież, M., Kuziak, A., Witek, K., Piska, K., Niemiec, D., Kasza,

P., Pękala, E. and Empel, J., 2023. Design and synthesis of novel arylurea derivatives of aryloxy (1-phenylpropyl) alicyclic diamines with antimicrobial activity against multidrug-resistant Gram-positive bacteria. European Journal of Medicinal Chemistry, 251, p.115224.

Ceramella, J., Iacopetta, D., Catalano, A., Cirillo, F., Lappano, R. and Sinicropi, M.S., 2022. A review on the antimicrobial activity of Schiff bases: Data collection and recent studies. Antibiotics, 11(2), p.191.

Chen, Y.; Mi, Y.; Li, Q.; Dong, F.; Guo, Z. Synthesis of Schiff bases modified inulin derivatives for potential antifungal andantioxidant applications. Int. J. Biol. Macromol. 2020, *143*, 714–723

Chowdhary, A.; Tarai, B.; Singh, A.; Sharma, A. Multidrug-resistant *Candida auris*infections in critically Ill coronavirus disease patients, India, April–July 2020. Emerg. Infect. Dis.2020,*26*, 2694.

Dassault Systemes BIOVIA. BIOVIA Discovery Studio Visualizer; v16.1.0.15350; Dassault Systemes: San Diego, CA, USA, 2015.

Devi, P., Singh, K. and Kubavat, B., 2023. Synthesis, spectroscopic, quantum, thermal and kinetics, antibacterial and antifungal studies: Novel Schiff base 5-methyl-3-((5-bromosalicylidene) amino)-pyrazole and its transition metal complexes. Results in Chemistry, 5, p.100813.

Dong, Y., Li, M., Hao, Y., Feng, Y., Ren, Y. and Ma, H., 2023. Antifungal Activity, Structure-Activity Relationship and Molecular Docking Studies of 1, 2, 4-Triazole Schiff Base Derivatives. Chemistry & Biodiversity, p.e202201107.

Elneairy, M.A., Sanad, S.M. and Mekky, A.E., 2023. One-pot synthesis and antibacterial screening of new (nicotinonitrile-thiazole)-based mono-and bis (Schiff bases) linked to arene units. SyntheticCommunications, 53(3), pp.245-261.

El-saied, F.A., Shakdofa, M.M., Al-Hakimi, A.N. and Shakdofa, A.M., 2020. Transition metal complexes derived from N′-(4-fluorobenzylidene)-2-(quinolin-2-yloxy) acetohydrazide: Synthesis, structural characterization, and biocidal evaluation. Applied Organometallic Chemistry, 34 (11), 5898.

El-Tabl, A.S., Shakdofa, M.M., Labib, A.A. and Al-Hakimi, A.N., 2012. Antimicrobial activities of the metal complexes of N′-(5-(4-chlorophenyl) diazenyl)-2-hydroxybenzylidene)-2-hydroxybenzohydrazide. Main Group Chemistry, 11(4), pp.311-327.

Erturk, A.G. Synthesis, structural identifications of bioactive two novel Schiff bases. *J. Mol. Struct.* **2020**, *1202*, 27299.

Frisch, M.J.; Trucks, G.W.; Schlegel, H.B.; Scuseria, G.E.; Robb, M.A.; Cheeseman, J.R.; Montgomery, J.A., Jr.; Vreven, T.K.K.N.; Kudin, K.N.; Burant, J.C.; et al. 2013. Gaussian 09, Revision D.01; Gaussian, Inc.: Wallingford, CT, USA.

Genchi, G.; Lauria, G.; Catalano, A.; Carocci, A.; Sinicropi, M.S. The double face of metals: The intriguing case of chromium. Appl.Sci. 2021,*11*, 638

Ghrab, S., Lahbib, K., Aroua, L. and Beji, M., 2017. Evaluation of antioxidant activity of selected new synthesized oxazolidin-2-one derivatives. Journal of the Tunisian Chemical Society, 19, pp.368-374.

Gümü¸s, A.; Okumu¸s, V.; Gümü¸s, S. Synthesis, biological evaluation of antioxidant-antibacterial activities and computational studies of novel anthracene-and pyrene-based Schiff base derivatives. Turk. J. Chem. 2020, 44, 1200–1215.

Gurubilli (2023). Synthesis, characterization, and biological evaluation of Ni, Co, and Cu Metal Complexes with Heterocyclic Compounds. Int J Pharm Chem, 7-11. https://doi.org/10.46796/ijpc.v4i2.445.

Hamad, A.; Chen, Y.; Khan, M.A.; Jamshidi, S.; Saeed, N.; Clifford, M.; Hind, C.; Sutton, J.M.; Rahman, K.M. Schiff bases of sulphonamides as a new class of antifungal agent against multidrug-resistant *Candida auris*. Microbiol. Open2021, *10*, 1218.

Hassan, A.S., Morsy, N.M., Aboulthana, W.M. and Ragab, A., 2023. Exploring novel derivatives of isatin-based Schiff bases as multi-target agents: design, synthesis, in vitro biological evaluation, and in silico ADMET analysis with molecular modeling simulations. RSC advances, 13(14), pp.9281-9303.

Hassan, A.S.; Askar, A.A.; Nossier, E.S.; Naglah, A.M.; Moustafa, G.O.; Al-Omar, M.A. Antibacterial evaluation, in silico characters and molecular docking of Schiff bases derived from 5-aminopyrazoles. *Molecules* 2019, *24*, 3130.

Heras-Mozos, R., Hernández, R., Gavara, R. and Hernández-Muñoz, P., 2022. Dynamic covalent chemistry of imines for the development of stimuli-responsive chitosan films as carriers of sustainable antifungal volatiles. Food Hydrocolloids, 125, p.107326.

Hosny, S., Ragab, M.S. and Abd El-Baki, R.F., 2023. Synthesis of a new sulfadimidine Schiff base and their nano complexes as potential anti-COVID-19 and anti-cancer activity. Scientific Reports, 13(1), p.1502.

Keche, A.P., Hatnapure, G.D., Tale, R.H., Rodge, A.H., Birajdar, S.S. and Kamble, V.M., 2012. A novel pyrimidine derivative with aryl urea, thiourea and sulfonamide moieties: Synthesis, anti-inflammatory and antimicrobial evaluation. Bioorganic & medicinal chemistry letters, 22(10), pp.3445-3448.

Kumari (2019). Antimicrobial Activity of Copper (II) and Cobalt(II) Complexes of Citral-Valine Derived Schiff Base. Asian J. Chem., 1(32), 192-194. https://doi.org/10.14233/ajchem.2020.21801

Layaida, H., Hellal, A., Chafai, N., Haddadi, I., Imene, K., Anis, B., Mouna, E., Bensouici, C., Sobhi, W., Attoui, A. and Lilia, A., 2022.Synthesis, spectroscopic

characterization, density functional theory study, antimicrobial and antioxidant activities of curcumin and alanine-curcumin Schiff base. Journal of Biomolecular Structure and Dynamics, pp.1-16.

Liang, X.X., Zhao, X.Y., Guo, A., Wang, X.W., Rong, M., Chang, L., Sun, Z.Q. and Jin, X.D., 2023. Synthesis, crystal structure and antibacterial activity of zinc (II) complexes with Schiff bases derived from 5-fluorosalicylaldehyde.Journal of Coordination Chemistry, pp.1-15.

Liang, X.X., Zhao, X.Y., Guo, A., Wang, X.W., Rong, M., Chang, L., Sun, Z.Q. and Jin, X.D., 2023. Synthesis, crystal structure and antibacterial activity of zinc (II) complexes with Schiff bases derived from 5-fluorosalicylaldehyde. Journal of Coordination Chemistry, pp.1-15.

Lotfi, A., 2020. Synthesis and characterization of novel mixed complexes derived from 2-aminomethylbenzimidazole and 2-(1H-Benzimidazol-2-yl) aniline and theoretical prediction of toxicity. Egyptian Journal of Chemistry, 63(12), pp.4757-4767.

Madani, S., Mokhnache, K., Rouane, A. and Charef, N., 2020. Synthesis, Characterization and In vitro evaluation of antibacterial and antifungal activities of New Schiff Base and Its Metal Complexes. Materials and Biomaterials Science, 3(1), pp.001-009.

Madani, S., Mokhnache, K., Rouane, A., Charef, N. 2020. Synthesis, Characterization and In vitro evaluation of antibacterial and antifungal activities of New Schiff Base and Its Metal Complexes. Mater. Biomater. Sci, 3, 001-009.

Magalhães, T.F.F.; da Silva, C.M.; Dos Santos, L.B.F.; Santos, D.A.; Silva, L.M.; Fuchs, B.B.; Mylonakis, E.; Martins, C.V.B.; de Resende-Stoianoff, M.A.; de Fátima, Â. Cinnamyl Schiff bases: Synthesis, cytotoxic effects and antifungal activity of clinicalinterest. Lett. Appl. Microbiol. 2020, *71*, 490–497.

Messasma, Z., Ourari, A., Mahdadi, R., Houchi, S., Aggoun, D., Kherbache, A. and Bentouhami, E., 2018. Synthesis, spectral characterization, DFT computational studies and inhibitory activity of novel N2S2 tetradentates Schiff bases on metallo-beta-lactamases of Acinetobacter baumannii. Journal of Molecular Structure, 1171, pp.672-681.

Morris, G.M.; Huey, R.; Olson, A.J. 2008. Using AutoDock for ligand-receptor docking. Curr. Protoc. Bioinform., 24, 8–14.

Oliveira, I.S., Manzano, C.M., Nakahata, D.H., Santiago, M.B., Silva, N.B.S., Martins, C.H.G., Respindula, F.P., Pereira, D.H. and Corbi, P.P., 2022. Antibacterial and antifungal activities in vitro of a novel silver (I) complex with sulfadoxine-salicylaldehyde Schiff base. Polyhedron, 225, p.116073.

Omer, A.M., Eltaweil, A.S., El-Fakharany, E.M., Abd El-Monaem, E.M., Ismail, M.M., Mohy-Eldin, M.S. and Ayoup, M.S., 2023.Novel Cytocompatible Chitosan Schiff Base Derivative as a Potent Antibacterial, Antidiabetic, and Anticancer Agent.Arabian Journal for Science and Engineering, pp.1-15.

Othman, I.M., Gad-Elkareem, M.A., Aouadi, K., Snoussi, M. and Kadri, A., 2021. New substituted pyrazolones and dipyrazolotriazines as promising tyrosyl-tRNA synthetase and peroxiredoxin-5 inhibitors: Design, synthesis, molecular docking and structure-activity relationship (SAR) analysis. Bioorganic chemistry, 109, p.104704.

Poonia, N., Lal, K., Kumar, A., Kumar, A., Sahu, S., Baidya, A.T. and Kumar, R., 2022. Urea-thiazole/benzothiazole hybrids with a triazole linker: synthesis, antimicrobial potential, pharmacokinetic profile and in silico mechanistic studies. *Molecular Diversity*, pp.1-17.

PrabhuKumar, K.M., Satheesh, C.E., RaghavendraKumar, P., Kumar, M.N.S., Lingaraju, K., Suchetan, P.A. and Rajanaika, H., 2022. Synthesis, characterization, antibacterial, antifungal and antithrombotic activity studies of new chiral selenated Schiff bases and their Pd complexes. Journal of Molecular Structure, 1264, p.133172.

Rezaei, M.T., Keypour, H., Hajari, S., Farida, S.H.M., Saadati, M. and Gable, R.W., 2023. Theoretical and solid-state structures of three new macroacyclic Schiff base complexes and the investigation of their anticancer, antioxidant and antibacterial properties. RSC advances, 13(14), pp.9418-9427.

Rezaei, M.T., Keypour, H., Hajari, S., Farida, S.H.M., Saadati, M. and Gable, R.W., 2023. Theoretical and solid-state structures of three new macroacyclic Schiff base complexes and the investigation of their anticancer, antioxidant and antibacterial properties. *RSC advances*, *13*(14), pp.9418-9427.

Rietveld, H.M. A profile refinement method for nuclear and magnetic structures. 1969, J. Appl. Cryst., 2, 65. doi.org/10.1107/S0021889869006558

Roopa, D.L., Shyamsunder, K., Karunakar, P., Ramalingam, R.J., Venkatesulu, A., Karnan, M., Kiran, K.S., Selvaraj, M. and Basavarajaiah, S.M., 2023. Naphtho [2, 1-b] furan derived triazole-pyrimidines as Highly potential InhA and Cytochrome c peroxidase inhibitors: Synthesis, DFT calculations, Drug-Likeness profile, molecular docking and dynamic studies. Journal of Molecular Structure, p.135685.

Rugaie, O.A., Mohammed, H.A., Alsamani, S., Messaoudi, S., Aroua, L.M., Khan, R.A., Almahmoud, S.A., Altaleb, A.D., Alsharidah, M., Aldubaib, M. and Al-Regaiey, K.A., 2023. Antimicrobial, Antibiofilm, and Antioxidant Potentials of Four Halophytic Plants, Euphorbia chamaesyce, Bassia arabica, Fagoniamollis, and Haloxylonsalicornicum, Growing in Qassim Region of Saudi Arabia: Phytochemical Profile and In Vitro and In Silico Bioactivity Investigations. Antibiotics, 12(3), p.501.

Saghatforoush, L.A., Chalabian, F., Aminkhani, A., Karimnezhad, G. and Ershad, S., 2009. Synthesis, spectroscopic characterization and antibacterial activity of new cobalt (II) complexes of unsymmetrical tetradentate (OSN2) Schiff base ligands. European journal of medicinal chemistry, 44(11), pp.4490-4495.

Salihovi´c, M.; Pazalja, M.; Halilovi´c, S.Š.; Veljovi´c, E.; Mahmutovi´c-Dizdarevi´c, I.; Roca, S.; Novakovi´c, I.; Trifunovi´c, S. Synthesis, characterization, antimicrobial activity and DFT study of some novel Schiff bases. J. Mol Struct.2021, 1241, 130670.

Salihović, M.; Pazalja, M.; Halilović, S.Š.; Veljović, E.; Mahmutović-Dizdarević, I.; Roca, S.; Novaković, I.; Trifunović, S. Synthesis, characterization, antimicrobial activity and DFT study of some novel Schiff bases. J. Mol Struct. 2021, 1241, 130670

Shakdofa, M.M., Morsy, N.A., Rasras, A.J., Al-Hakimi, A.N. and Shakdofa, A.M., 2021. Synthesis, characterization, and density functional theory studies of hydrazone–oxime ligand derived from 2, 4, 6-trichlorophenyl hydrazine and its metal complexes searching for new antimicrobial drugs. Applied Organometallic Chemistry, 35 (2), 6111.

Sharma, B.P., Subin, J.A., Marasini, B.P., Adhikari, R., Pandey, S.K. and Sharma, M.L., 2023. Triazole based Schiff bases and their oxovanadium (IV) complexes: Synthesis, characterization, antibacterial assay, and computational assessments. Heliyon.

Shaygan, S., Pasdar, H., Foroughifar, N., Davallo, M. and Motiee, F., 2018. Cobalt (II) complexes with Schiff base ligands derived from terephthalaldehyde and ortho-substituted anilines: Synthesis, characterization and antibacterial activity. applied sciences, 8(3), p.385.

Sroor, F.M., Othman, A.M., Aboelenin, M.M. and Mahrous, K.F., 2022. Anticancer and antimicrobial activities of new thiazolyl-urea derivatives: Gene expression, DNA damage, DNA fragmentation and SAR studies. *Medicinal Chemistry Research*, *31*(3), pp.400-415.

Tallet, L., Frisch, E., Bornerie, M., Medemblik, C., Frisch, B., Lavalle, P., Guichard, G., Douat, C. and Kichler, A., 2022. Design of Oligourea-Based Foldamers with Antibacterial and Antifungal Activities. *Molecules*, *27*(5), p.1749.

Trott, O.; Olson, A.J. 2010 AutoDock Vina: Improving the speed and accuracy of docking with a new scoring function, efficient optimization, and multithreading. J. Comput. Chem., 31, 455–461.

Uddin, T.M., Chakraborty, A.J., Khusro, A., Zidan, B.R.M., Mitra, S., Emran, T.B., Dhama, K., Ripon, M.K.H., Gajdács, M., Sahibzada, M.U.K. and Hossain, M.J., 2021. Antibiotic resistance in microbes: History, mechanisms, therapeutic strategies and future prospects. Journal of infection and public health, 14(12), pp.1750-1766.

Varshney, A. and Mishra, A.P., 2023. Synthesis, spectral characterization, computational studies, antifungal, DNA interaction, antioxidant and fluorescence property of novel Schiff base ligand and its metal chelates. Spectrochimica Acta Part A: Molecular and Biomolecular Spectroscopy, p.122765.

Wang, C., Fan, L., Pan, Z., Fan, S., Shi, L., Li, X., Zhao, J., Wu, L., Yang, G. and Xu, C., 2022. Synthesis of Novel Indole Schiff.Base Compounds and Their Antifungal Activities. Molecules, 27(20), p.6858.

Yusuf, T.L.; Oladipo, S.D.; Olagboye, S.A.; Zamisa, S.J.; Tolufashe, G.F. Solvent-free synthesis of nitrobenzyl Schiff bases: Characterization, antibacterial studies, density functional theory and molecular docking studies. J. Mol. Struct. 2020, 1222, 128857.

Zha, L., Xie, Y., Wu, C., Lei, M., Lu, X., Tang, W. and Zhang, J., 2022. Novel benzothiazole–urea hybrids: Design, synthesis and biological activity as potent anti-bacterial agents against MRSA. European Journal of Medicinal Chemistry, 236, p.114333.